Nonlinear Phenomena in Complex Systems, vol. **11**, no. 2 (2008), pp. 198 - 204

A New Dripping Faucet Experiment

C. E. Somarakis,* G. E. Cambourakis,† and G. P. Papavassilopoulos‡
School of Electrical and Computer Engineering,
National Technical University of Athens, GREECE
(Received 5 December, 2007)

A dripping faucet experiment, based on a new apparatus is presented. Time-drop intervals, covering the entire dripping spectrum, are measured and a multifarious nonlinear action is detected. In particular, we report three distinct dripping regions of complex behavior and discuss their main features. Finally, we propose alternative methods for estimating the invariant characteristics of the experimental signals, in frames of nonlinear time series analysis.

PACS numbers: 47.52.+j; 05.45.Tp
Keywords: chaos, nonlinear analysis, time series, dripping faucet

1. Introduction and historical notes

A dripping faucet may easily be seen in everyday life. Its rhythm depends, sensitively, on the flow of water and can be either regular or irregular. In the latter case, one might blame it on noise due to unseen influences such as small air vibrations. However, it is nowadays well-known that dripping faucet is a paradigm of a dissipative nonlinear physical system capable of exhibiting chaos. The same system can change from a periodic and predictable to an aperiodic, quasi-random pattern of behavior, as a single parameter (in this case, the flow rate) is varied.

The story of drips falling from a faucet goes back, in the early 70's. At the dawn of this decade, it had been generally realized that simple mechanical oscillators can undergo a transition from predictable to unpredictable behavior analogous to the transition from laminar to turbulent flow in a fluid. In 1977, O. Rössler suggested that an exceptional connection between flow and oscillator dynamics is the example of a dripping faucet [1]. R. Shaw *et al*, ([2, 3]) were the first who, in 1984, studied this phenomenon experimentally, proving Rössler's suggestion true and establishing the aspect that Chaos is not only a mathematical product but also a phenomenon ubiquitous in the real world. In the years to follow, there had been other similar attempts (see Ref. [4–6]).

1.1. The Experimental Apparatus

Water from a large tank (*50x50x20 cm*) is metered trough a valve to a nozzle with orifice of *4mm* diameter. Drops fall from the orifice, break a laser beam and generate pulses in a photocell signal (see Fig.1). The signal is guided through an analog device to a computer where it is digitized. In the end, the signal we receive is a sequence of pulses adjusted to drops. What we measure is the time distance between consecutive peaks, which corresponds to the time distance between consecutive drops. This sequence of numbers, $\{T_n\}$, is the the apparatus' output signal in which, study and analysis of its behavior, in frames of nonlinear dynamic systems theory, is carried out. The control of the system is the rate of drops, which we will meet throughout this paper. It will be symbolised by f and measured in *drops/sec* units. The experiment's main specifications are: Hydrostatic pressure $\simeq 0.98$ atm and environment's temperature at 20 to 25 ^oC. For further information on the experimental setup, see Ref. [7].

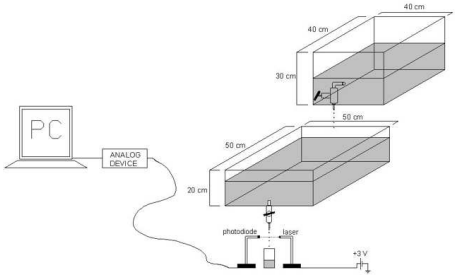

FIG. 1. Diagram of the experimental apparatus. The main tank generates drips to be detected by the laser system while the secondary tank keeps the main tank's hydrostatic pressure steady.

*E-mail: cslakonas@yahoo.gr
†E-mail: gcamb@cs.ntua.gr
‡E-mail: yorgos@netmode.ntua.gr

2. Results and Discussion

The project is separated in two sections. The first one is the view of the various signals from the entire data spectrum that our water system can generate. Varying the flow rate (drops/sec), which is our only control parameter, we observe the recorded signals and attempt through visual inspection, to clarify these behaviors.

The second part of our paper is the analysis of certain output signals implementing more elaborate techniques of nonlinear time-series analysis (see Ref. [8–10]). The main strategy is based on modelling our experimental time-series and generate artificial data capable of providing numerical estimations of some basic characteristic invariant quantities of chaos in the dynamical systems, such as Correlation Dimension, Correlation Entropy and Maximal Lyapunov Exponent.

2.1. Nonlinear Phenomena and Chaos

A typical recording of the phenomenon's evolution, provides us with a sequence of numbers that, as it is stated above, is approximately, the time between successive drops. The most common method for inspecting such streams of numbers, is the method of delay plots (T_n, T_{n+1}), which is capable of verifying possible deterministic connection between consecutive drop intervals. These delay plots can be considered as Poincaré planes of an underlying continuous dynamic system ([2, 4, 8]). Apart from these maps, we will also make use of the regular time-series plots (n, T_n),when necessary. Along with delay plots, they are the most powerfull tool for the understanding of such dynamic evolution. In our experiment, three sorts of signals were observed. This is how the necessity to roughly outline, equal in number, dripping zones, has emerged. We cited these discreet regions as:

- *The 2D Low Dimensional Chaos*
- *The Nebulous Zone*
- *The 3D Low Dimensional Chaos.*

2.1.1. 2D Low Dimensional Chaos

This family of attractors is defined for dripping rates not higher than f=3.5 drops/sec. This is a highly unstable zone, where many nonlinear phenomena coexist with chaos. Typical output signals of this region are most probably to depict long-term transients or intermittencies from periodic to chaotic patterns. As far as the purely chaotic time-series are concerned, these, generally, converge to strange attractors which lie on two-dimensional manifolds. In other words, *hénon-like* attractors, are the types of chaotic limit sets to be observed. These attractors have also been observed [2, 5, 11]. In following figures, we will introduce various experimental time-series of this zone. Furthermore, we will present a phenomenon, sufficiently, interpreted in frames of a crisis.

Periodic Patterns

Undoubtedly, orbits in this region are not prone to a regular evolution and thus, periodic patterns are rarely observed. All in all, we observed periodic solutions of period one, two, three and four. In Fig. 2, below, we present a characteristic signal exhibiting at f=2.43 drop/sec a period-3 behavior, at first, and through an abrupt transition, period-1 orbits at f=2.53 and 2.54 drop/sec. Despite the dominating periodicity here, the silhouette of a "worm-like"attractor, existing nearby period-3 orbit, is easily noticed.

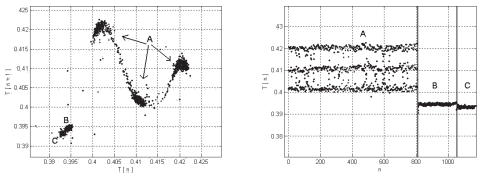

FIG. 2. Periodic Patterns. Left image (T_n, T_{n+1}): delay-plot, right image (n, T_n): time-series. This signal exhibits regular behavior of period 3 and then 1. For the period-3, A-noted, interval the estimated rate is f=2.43 drops/sec while for the rest period-1, B and C-noted,intervals where f=2.53 and 2.54 drops/sec, respectively.

Transient State

In lower dripping rates, like here, the transition of a typical orbit to steady state may sometimes be a generally lengthy procedure. Our system takes significant amount of time, in order to eliminate trend and settle down to steady state. The value of transients in our experiment is that the orbit is for a long time attracted by the neighboring limit sets, before settling down to the steady state attractor. This discloses the contigious, to the steady state attractor, dynamics. In Figs. 3 and 4 we present two of the most common kinds of transients. Hence, for example in Fig. 3 the steady state can be readily identified to be the period-1 orbit around T≈0.65 sec. However,

the orbit starts from T≈0.605 sec and in it's effort to reach the steady state, is attracted, firstly, by a limit cycle and then by a strange attractor. It can be, therefore, concluded that a limit cycle and a strange attractor exist in the dripping rate interval between 1.54 and 1.65 drops/sec. Another transient

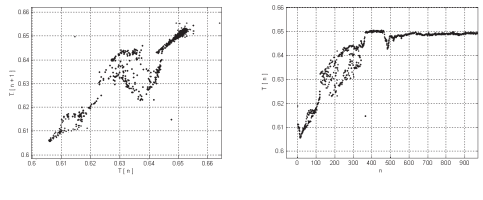

FIG. 3. Transient Mode. Left image (T_n, T_{n+1}): delay-plot, right image (n, T_n): time-series. In it's run to steady state, this signal "indulges"in conterminious basins of attraction of different limit sets. Finally, it settles down to period one where f=1.54 drops/sec.

state is presented in Fig. 4. In this case, the signal varies among three different chaotic attractors. It is worth noticing that these attractors do not intersect to each other. Especially B and C limit sets present a remarkable symmetry.

The feature of transient mode is, exclusively, observed

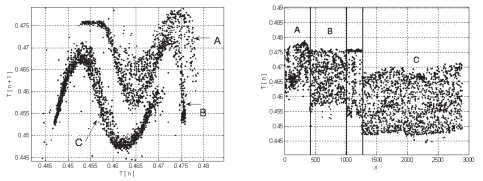

FIG. 4. Transient Mode. Left image (T_n, T_{n+1}): delay-plot, right image (n, T_n): time-series. In the recording above, the orbit is confined in the A-noted region at rate f=2.13 drops/sec, then suddenly jumps to a chaotic mode with no trend in the B-noted region where f=2.14 drops/sec. Finally, the trajectory enters the C-noted interval, where a strange attractor emerges. For this, dripping rate is calculated to be f=2.19 drops/sec.

in this dripping zone, whereas in the rest two zones no such states were noticed. We shall continue, now, to some purely chaotic signals, many of which have been also detected in previous works (see Ref. [2, 3, 5, 6]).

Strange Attractors

The expected result of any dripping faucet experiment is of course delay-plots that resemble to figures like these of Figs.5 to 7. These *worm-like* figures are now considered to be nothing more than limit sets topologically similar to a 2D logistic or Hénon attractor. Here we present our apparatus', lower dripping rate, chaotic signals. This sort of attractors is only detected in this dripping zone. In the other regions, much more complicated attractors come to view. In the meantime, for f=1.84 drops/sec we will observe an attractor pretty similar to this of Fig. 5. For f=1.97 drops/sec a strange set same as this of Fig.

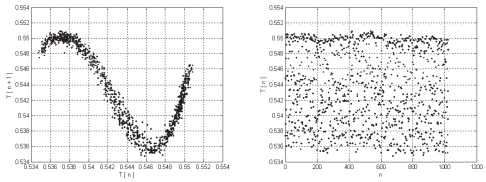

FIG. 5. Chaotic Attractor. Left image (T_n, T_{n+1}): delay-plot, right image (n, T_n): time-series. Dripping rate f=1.84 drops/sec.

6 is about to appear and for f=2.68 drops/sec another attractor, similar to this in Fig. 7, may be discerned. In the second part of this paper we will work on these

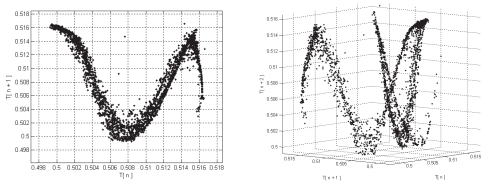

FIG. 6. Chaotic Attractor. Left image (T_n, T_{n+1}): 2D delay-plot, right image (T_n, T_{n+1}, T_{n+2}): 3D delay-plot. Dripping rate f=1.97 drops/sec.

two signals again in a more innovative way.

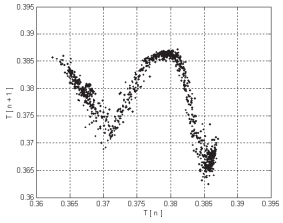

FIG. 7. Chaotic Attractor. Image (T_n, T_{n+1}): delay-plot. Dripping rate f=2.65 drops/sec.

A double boundary crisis

In this section we will present a sequence of signals recorded at the region of 2.67 drops/sec. The system, here, exhibits an obscure behavior, which however, can sufficiently be clarified as a type of boundary crisis. We

begin our analysis, by examining the graph in Fig. 8 where f=2.66 drops/sec. The attractor appears to be splitted in two compartments. This structure can be detected by speculating a window of our time-series (n,T_n) plot, presented in Fig. 8. Apparently, the orbit oscillates between the two fragments going through a chaotic mode in every part. The strange attractor consists of these two parts which we have distinguished with a curve (see Fig. 8). This chaotic mode comes

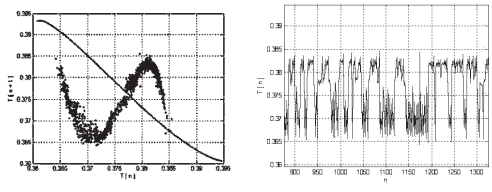

FIG. 8. First stage of a nonlinear phenomenon related to a crisis. Left image (T_n, T_{n+1}): delay-plot, right image (n, T_n): time-series. Here f=2.66 drops/sec, where a two-sided chaotic attractor comes to rise. In the right image, the signal is printed in continuous form, for convenience.

to a halt for f=2.67 drops/sec and a period-2 orbit supplants the previous attractor, as we can see in Fig. 9. The periodic behavior seizes for f=2.69 drops/sec,

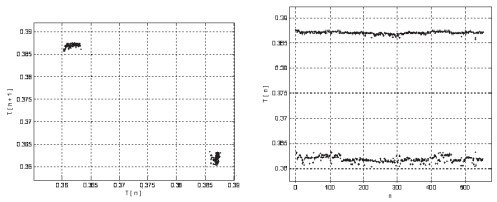

FIG. 9. Second stage of a nonlinear phenomenon related to a crisis. Left image (T_n, T_{n+1}): delay-plot, right image (n, T_n): time-series. Here f=2.67 drops/sec. Abrupt transition from chaos to period-2 mode.

where a new strange attractor appears. In Fig. 10 we can notice it's form and magnitude. This attractor is considerably bigger than that of Fig. 8 and obviously in a uniform connected structure. The string of signals presented above may thought to be consecutive regular intermittencies between order and chaos. This is, however, a less probable scenario. The same pattern of behavior has been detected in the Chua Circuit (see Ref [12]).

2.1.2. Nebulous Zone

This family of attractors is defined for dripping rates between 3.5 drops/sec and 12 drops/sec. At

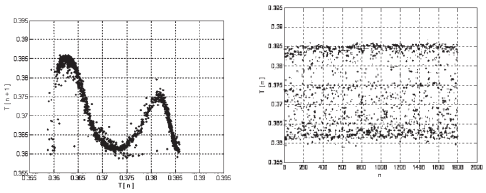

FIG. 10. Third stage of a nonlinear phenomenon related to a crisis. Here f=2.69 drops/sec. Abrupt transition from period-2 mode to chaos.

these dripping rates we meet schemes like these in Figs. 11 and 12. We call this zone *Nebular* in order to depict the withering of deterministic chaos. This world consists of vague figures that, although seem resemblant to strange attractors, they exhibit no pure chaotic behavior [7]. A possible explanation is that, at this dripping span, a debilitation in the oscillatory character of drops may occur. For example, an attenuation of resonance between the water particles. It is also likely that typical trajectories of this zone are, in fact, hybrid; consisting of both deterministic and stochastic features. In such case, a typical orbit alters from chance to chaos in an irregular, maybe chaotic, manner. Nevertheless, further research, in order to gain a more concrete perspective for the dynamics of this zone, has to be done.

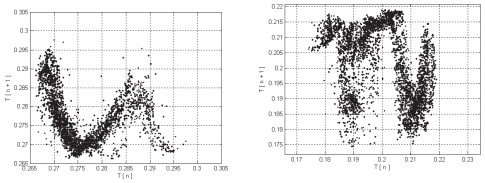

FIG. 11. Attractors of Nebulous Zone. (T_n, T_{n+1}) delay-plots: The left one depicts a signal of f=3.61 drops/sec, whereas the right one, a signal of f=5.02 drops/sec.

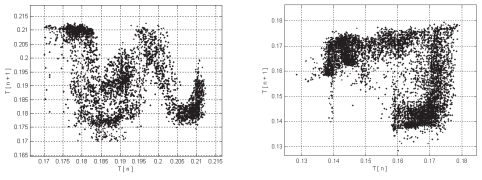

FIG. 12. Attractors of Nebulous Zone. (T_n, T_{n+1}) delay-plots: The left one is a signal of f=5.21 drops/sec, whereas the right one is recorded at f=6.29 drops/sec.

2.1.3. 3D Low Dimensional Chaos

This is the third and last dripping region, that is defined for f=12 drops/sec to f=23 drops/sec. Here, novel and more complicated strange attractors appear. As has already been noted [2, 3], these objects are not sufficiently defined in plane return-maps. Here we reconstruct them in 2D maps for convenience reasons, only. Analysis of these signals, in order to determine the nature and type of chaos showed that these objects lie in a 3D manifold and sufficiently defined by a 3D dynamic spectrum of Lyapunov exponents, only one of which has a positive sign (see ref [2, 7]). This is, actually, the reason for which both third and first zone, are named after. In the 3D Low Dimensional Chaos dripping area, chaotic mode is, virtually, omnipresent. Attractors appear to be remarkably big and of high complexity. Nevertheless, there are, rather, few nonlinear phenomena. Transition between attractors is rather smooth with few intermittencies, whereas periodic behavior was scarcely detected. Furthermore, neither transient mode, nor trends or any other instability as in the first zone, was observed (for more see Ref. [7]). In the next four figures we present the main strange attractors, that were detected in this region. In Fig. 16 we plot the 3D representation (T_n,T_{n+1},T_{n+2}) of the time-series of Fig. 15 (see respective figures for further details).

At this point, the representation and inspection of some characteristic signals from our experiment, is completed. Dripping turns to jetting for rates higher than 23 drops/sec. For even higher dripping rates experimental equipment of larger capacity is required. (one can see ref [5, 11]). We now pass on to a new method for studying our data.

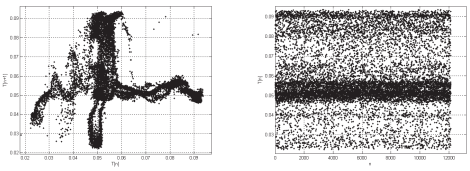

FIG. 13. Strange Attractors of 3D Low Dimensional Zone. Left image (T_n, T_{n+1}): delay-plot, right image (n, T_n): time-series. Here f=16.78 drops/sec.

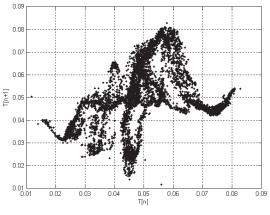

FIG. 14. Strange Attractors of 3D Low Dimensional Zone. Image (T_n, T_{n+1}): delay-plot. Here f=20.83 drops/sec.

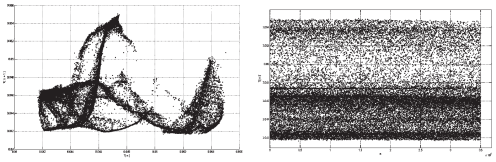

FIG. 15. Strange Attractors of 3D Low Dimensional Zone. Left image (T_n, T_{n+1}): delay-plot, right image (n, T_n): time-series. This attractor has also been found in previous works (see Ref. [2]) Here f=22.5 drops/sec.

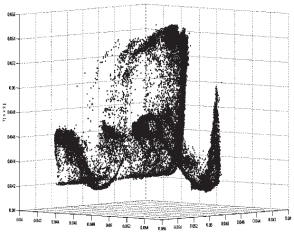

FIG. 16. Strange Attractors of 3D Low Dimensional Zone. 3D reconstruction of the signal in Fig. 15 in (T_n, T_{n+1}, T_{n+2}) phase space.

2.2. Nonlinear Modelling

2.2.1. Modelling Strategy

The rudimentary assumption on which the dripping faucet research is based, is that, whatever the underlying continuous dynamic system is, the time intervals between successive drops are,virtually, numbers generated by a map-equation of the form:

$$x_{n+1} = f(x_n). \tag{1}$$

From this point of view, one would try to estimate this function f and generate data with similar to the real data statistical features. More information concerning prediction and modelling of time-series can be found here [8–10]. Back to our experiment, now, we made use of a certain nonlinear model.

Radial Basis Functions

This is a very flexible class of global nonlinear models. According to this modelling strategy, function (1) can

estimated by a linear superposition of basis functions

$$x_{n+1} = F(x_n) = a_0 + \sum_{i=1}^{n} a_i \Phi_i(d(x_n, y_i)) \qquad (2)$$

where $\Phi(r)$ are bell-shaped functions with a maximum at $\Phi(0)$ and a rapid decayed towards zero with increasing r. The argument of Φ_i is a metric function of x_n and a selected point y_i on the attractor. For more information concerning (2) see Ref [8, 9, 13].
The necessity for modelling our data came from the fact that the apparatus generates both noisy and statistically poor time-series. It is obvious that no valid numerical analysis of a sequence of number with length less than 3000 points, can be executed. On the other hand, successful modelling generates arbitrarily long and noise-free stream of numbers which are statistically close to our real data. In such case, an assiduous analysis of our surrogate time-series can lead to handfull results concerning our real system. The implemented algorithm worked remarkably well for pure chaotic signals of the 2D Low Dimensional Chaos zone, contrary to the rest dripping zones where the results were disappointing.

In Figs. 17 and 18 we present the delay plots (T_n, T_{n+1}) of artificial time-series based on the real signals of Fig.5 and 6, respectively. A rough visual inspection can verify the resemblance of these signals. It is worth noticing that the Fig.5 shows a time-series of 1000 points the corresponding figure (Fig. 17) consists of 60000 points. Finally, in Fig. 19 one can compare and contrast real and modelled time-series of Fig. 6 and 18 in 3D delay plots.

2.2.2. Invariant Measures

The characterisation of deterministic chaos is not only a matter of visual inspection of the plots. Certain criteria have to be fullfilled such as exponential divergence of nearby trajectories and fractality in the geometry of the limit sets in the state space of typical solutions. In Ref. [7] we examine our modelled data thoroughly, in order to provide tangible evidence for the chaotic nature of stationary signals in low-dripping rates. Thus, by implementing certain algorithms [14], we have numerically estimated invariant quantities, the main of which are correlation integrals and Lyapunov exponents. In this paper, we present the main results from our analysis from the time-series of Fig. 18. In Fig. 20 graphs from correlation sums are presented. From the local slopes of different embedding dimensions, we would read off an estimate of correlation dimension $D_c = 1.48 \pm 0.01$ and correlation entropy $h_2 = 0.34 \pm 0.02$.

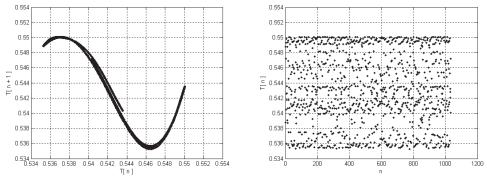

FIG. 17. RBF model of signal in Fig. 5. Left image (T_n, T_{n+1}): delay-plot, right image (n, T_{n+1}): time-series.

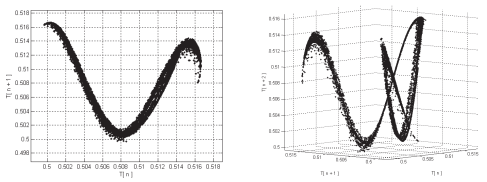

FIG. 18. RBF model of signal in Fig. 6. Left image (T_n, T_{n+1}): delay-plot, right image (T_n, T_{n+1}, T_{n+2}): 3D delay-plot.

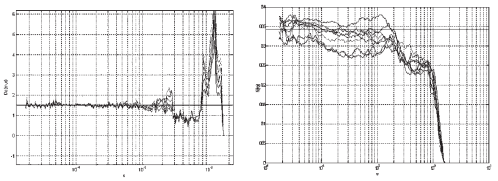

FIG. 19. Estimates of correlation dimension (left) and correlation entropy (right) of signal in Fig.6 (f=1.97 drops/sec). The correlation sum has been computed for embedding dimensions m=2,...,10. For the spatial ε-range scaling plateaus are detected leading to values $D_c = 1.48 \pm 0.01$ and $h_2 = 0.34 \pm 0.02$, respectively.

3. Conclusions

In this paper, a new experimental apparatus for the study of the classic dripping faucet system is presented. The equipments' stability, as well as the accuracy of the recordings, allowed an extended study of the system's dripping spectrum, the bandwidth of which is approximately 23 drops/sec. Three roughly distinct dripping zones were defined and various dynamics and phenomena were reported for each region separately. The first one, named 2D Low Dimensional Chaos, corresponding to lower dripping

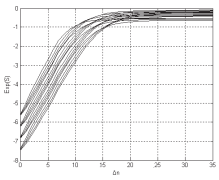

FIG. 20. Estimation of signal signal of Fig. 6. The embedding reconstructions vary from m=2,...,5 and the linear parts of the ccurves are well described by and exponential $\propto e^{0.49\Delta n}$. The estimation of maximam Lyapunov Exponent is $\lambda = 0.49 \pm 0.01$.

rates is a zone of many nonlinear phenomena that coexist together with chaos. One of them, conistent with a boundary crisis interpretation is outlined. Hénon-like types of limit sets were also observed. The next dripping zone, named Nebulous Zone, is an unclear region of not purely chaotic dynamics. It's attractors although seem to be strange, there are still no concrete evidence in favor of this view. Finally, the last family,named 3D Low Dimensional Chaos, is a world of large and complicated strange attractors which lie in 3D manifolds. In the last part of the paper a new perspective in studying our experimental data is proposed. Global nonlinear fitting models of radial basis functions were used to generate artificial time-series, qualitatively similar to the ones observed at the laboratory. This allowed a more profound research upon our experimental data in characterizing the nature and quantitative interpretation of deterministic chaos. A comprehensive analysis of these models is carried out in Ref. [7].

References

[1] O. Roessler, in *Synergetics : A Worhshop*, edited by H. Haken (Springer - Verlag, Berlin, 1977).

[2] R. Shaw, *The Dripping Faucet as a Model Chaotic System* (Aerial Press, Santa Cruz, CA, 1984).

[3] P. S. P. Martien, S. Pope and R. Shaw, Phys. Lett **A**, 399 (1985).

[4] Z. S. X. Wu, Physica D **40**, 433 (1989).

[5] W. G. J.C. Sartorelli and R. Pinto, Physical Review E **49**, 3963 (1994).

[6] F. P. A. D'Innocenzo and L. Renna, Physical Review E **65**, 056208 (2002).

[7] C. Somarakis, Master's thesis, School of Electrical and Computer Engineering (N.T.U.A.), Greece (2007), URL `http://artemis.cslab.ntua.gr:80/Dienst/UI/1.0/Display/artemis.ntua.ece/DT2007-0045`.

[8] H. Kantz and T. Schreiber, *Nonlinear Time Series Analysis* (Cambridge University Press, UK, 2005).

[9] M. Casdagli, Physica D **35**, 335 (1989).

[10] J. Eckmann and D. Ruelle, Physical Review Letters **57**, 617 (1985).

[11] W. J. Sartorelli and R. Pinto, Physica A **291**, 244 (2000).

[12] T. S. K. Alligood and J. Yorke, *CHAOS. An introduction to dynamical systems* (Springer, NY, 1996).

[13] D. Broomhead and D. Lowe, Complex Systems **2**, 321 (1988).

[14] H. K. R. Hegger and T. Schreiber, CHAOS **9**, 413 (1999).